# in vivo Sodium Imaging of Mouse Kidney at 9.4 Tesla: A Feasibility Study

H. Liu[1], M. G. Kohler[1], X. Shen[1], M. L. Garcia[1], D. S. Williams[2], R. J. Hargreaves[2]

[1]Merck Research Labs, Rahway, NJ, United States, [2]Merck Research Labs, West Point, PA, United States

INTRODUCTION: Among all MRI-observable elements in the biological system, sodium is the second most abundant element after hydrogen. Under normal physiological conditions the intracellular and extracellular sodium concentration in living tissue is approximately 15mM and 145mM, respectively. This large ionic concentration gradient across the cellular membrane in tissues is maintained dynamically by the Na-K pump on the cell membrane that consumes ATP. The failure of the Na-K pump due to impaired ATP production will lead to a significant increase in the intracelluar sodium concentration. Tissue sodium concentration has been exploited as an important indicator of the pathological status of tissue as well as a potential predictor of its fate during an ischemic event or degeneration or other pathological development (1-2). Interestingly, in the kidney, there exists another large corticomedullary sodium concentration gradient at the organ level, which is important for normal renal function. This unique feature of the kidney is essential for the counter-current and the urinary concentration mechanism. It is known that 23Na-MR imaging offers a unique approach to measure tissue sodium concentration non-invasively. Recently, an imaging technique was demonstrated for mapping kidney sodium distribution in rat by Maril et al (3). Driven by the availability of genetically engineered knock-out mice models, mice have been widely used in modern medical research as ideal and practical in vivo systems for studying various human diseases and their therapies. There is a need to develop efficient imaging methods for in vivo imaging in mice. The main aim of the study was to develop and evaluate the feasibility of 23Na MRI in mice with the kidney as the organ of interest. Since furosemide inhibits the coupled Na+/K+/2Cl- transport system in the luminal membrane of the thick ascending limb of the loop of Henle, the loop diuretics reduce the reabsorption of NaCl into the interstitium in outer medulla and then abolish this sodium concentration gradient. Another aim of the study was to validate the result by measuring the sodium concentration change induced by the loop diuretic in mouse kidney.

METHODS: Experiments were carried out on a 9.4-T/31-cm Bruker Biospec system (Ettlingen, Germany) and a 6-cm efficient gradient insert (maximum gradient strength =40G/cm; rise time = 80usec). A home-made two-turn circular RF coil (105.9MHz) was used as a Tx/Rx sodium and a linear birdcage coil was used to acquire proton images as anatomical reference. Decoupling between the two coils was achieved geometrically through maintaining the orthogonality between the B1 polarizations of the two coils. 23Na MRI pulse sequence consisted of a 3D gradient-echo (GE) acquisition scheme, in which a short RF pulse (200usec) was used to minimize unwanted magnetization relaxation processes during imaging. Other scan parameters: TR/TE=75/0.90msec, flip angle=90, NSA=16-32, echo asymmetry=20%. The spatial resolution parameters of the volumetric image set were: matrix of 64x32x16 corresponding to field of views of 64x48x32mm3. Typical scan times were ~ 20 min. C57/BL6 mice (n=7) were anesthetized mice with isofluorane (1.0-1.5% iso/air) using a nose cone at flow rate of 1 liter/min. After a base line 23Na MRI acquisition, a furosemide (15mg/kg, iv) bolus was injected via a jugular vein cannula 2 minute prior to the second 23Na MRI. In order to estimate RF non-uniformity of the coil, the excitation and reception field maps were measured experimentally. And, the transverse relaxation time (T2) was measured using a multiple echo version of the volume imaging sequence.

RESULTS: Representative proton and sodium images of mouse kidney are shown below (Fig.1A and B). The resulting image clearly revealed a sodium concentration gradient along the corticomedullary axis in kidney. The sodium concentration gradient in kidney was attenuated with the administration a known loop diuretic, furosemide. Fig. 1C shows the sodium concentration profiles across the kidney prior to and immediately after the diuretic injection. Approximately 50% decrease in outer medulla region was observed. Also, the resulting RF field of the probe was found to be substantially uniform over region of interest (variation less than 20%). The fast and slow T2* were found to be 2.0 and 21 msec.

CONCLUSIONS: The experimental results clearly suggest that the sodium imaging of mouse kidney is feasible and potentially practical using a high field NMR scanner. And, the added SNR at 9.4 Tesla allows high resolution imaging with voxel volume as small as 3 micro-liter in reasonable scan time. More importantly, both spatial resolution and SNR of the sodium images were sufficient for resolving the sodium concentration gradient and its change after a 15mpk flurosemide injection in mouse kidney. The result of the study suggests that such a non-invasive imaging based assessment can be used to gain insights regarding to renal function and mechanism of diuretics.

REFERENCES: 1. Kim RJ, et al. Fast 23Na Magnetic Resonance Imaging of Acute Reperfused Myocardial Infarction: Potential to Assess Myocardial Viability. Circulation 1997; 95: 1877-1885.

2. Thulborn KR, Gindin TS, Davis D, Erb P. Comprehensive MR imaging protocol for stroke management: tissue sodium concentration as a measure of tissue viability in nonhuman primate studies and in clinical studies. Radiology 1999; 213:156-166.

3. Maril N, Margalit R, Mispelter J, Degani H. Sodium magnetic resonance imaging of diuresis: Spatial and kinetic response. Magn Reson in Med 2005; 53: 545 – 552.

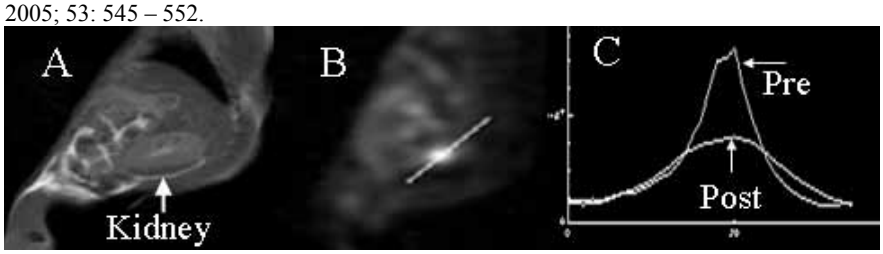


**Figure 1**. Water (A) and sodium (B) images of a mouse kidney taken immediately prior to a furosemide injection (15mpk). The sodium concentration profiles across the kidney before and after the injection were shown in C (the spatial location indicated in B).